

## Ionic Transport and FTIR Properties of Lithium Iodide Doped Biodegradable Rice Starch Based Polymer Electrolytes

M. H. Khanmirzaei, S. Ramesh\*

Centre for Ionics University of Malaya, Department of Physics, Faculty of Science, University of Malaya, 50603 Kuala Lumpur, Malaysia.

\*E-mail: [rameshtsubra@gmail.com](mailto:rameshtsubra@gmail.com)

Received: 29 April 2013 / Accepted: 14 June 2013 / Published: 1 July 2013

Biodegradable polymer electrolyte systems of Rice Starch-Lithium Iodide (RS-LiI) films were prepared using solution casting method. At room temperature, RS:LiI film with ratio of 65 wt.%:35 wt.% demonstrates the highest ionic conductivity of  $4.68 \times 10^{-5}$  S cm<sup>-1</sup>. Temperature-dependence ionic conductivity study follows Arrhenius model and using related plot, activation energy for highest conducting composition is 0.41 eV. The ac conductivity of each film is increased with increase in LiI content. Dielectric properties of mobility, diffusion coefficient, number density of mobile ions (Li<sup>+</sup>) and number of transitions per unit time were determined using Rice and Roth model. At higher conductivity, dielectric parameters were increased due to more mobile ions. The structure of polymer electrolytes was characterized by FTIR spectroscopy. Infrared spectra of compositions exhibited band shifts at different salt ratios. These shifts confirm complexation between host and salt.

**Keywords:** Polymer electrolyte; Ionic conductivity; Biodegradable Rice starch; Electric mobility; FTIR.

### 1. INTRODUCTION

Biodegradable polymers have economic and environmental benefits due to cheap in cost and biodegradability. Utilizing environmental friendly polymers in polymer electrolytes and electronics field can be good replacement for some harmful existing materials and admirable category for green energy applications such as solar cells, specifically, dye sensitized solar cells, super capacitors, batteries, etc.

Biodegradable polymers have greatly involved in many applications [1-18] with no harm for environment. Currently, biodegradable polymer electrolytes have applications in rechargeable lithium batteries [19-21], solar cells [22], dye sensitized solar cells [23], supercapacitors [24], and fuel cells

[25]. Among biodegradable polymers, natural polymers like starch has wide range of applications in drug delivery [26-32], food packaging [33] and medicine [34]. Starch based polymer electrolytes [24, 35-42] and even rice starch based polymer electrolytes [43-47] have impressive investigations on conductivity, rheological, structural and thermal properties and applications. One of the biggest challenges in polymer and salt complex is getting higher conductivity film. Some attempts to increase conductivity [48-50] show importance of salt on performance of conduction. Kobayashi et al. [51] reported that several lithium salt and salt content deeply affected the ion conductivity characteristics. Consequently, attempts to get better conductivity between different polymers and salts are still in progress. In this work, rice starch from starch group was used as fairly studied in literatures, and lithium iodide was used to examine new possible properties on conductivity, and dielectric parameters, and to develop future works in dye sensitized solar cell application [52] to evaluate performance and efficiency. In further studies, conductivity in this work can increase with other additives such as ionic liquids and fillers [53, 54].

The present work reports enhancement of ionic conductivity as a result of ion transport with  $\text{Li}^+$  ions after LiI complexation with RS. Other goals of this work focus on calculation of activation energy, number density of mobile ions, mobility, diffusion coefficient and transitions per unit time. Comparison between dielectric parameters which contribute to conductivity in different salt ratio at room temperature and higher temperatures will be widely discussed. FTIR analysis is discussed for samples in various salt contents. Furthermore, as dye sensitized solar cells need reversible  $\text{I}^3-/ \text{I}^-$  redox [55], this work has future work due to existence of  $\text{I}^-$  ion in lithium iodide salt which can create mentioned redox with iodine.

## 2. EXPERIMENTAL

### 2.1. Materials

Rice starch (Sigma-Aldrich) was used in this work without further purification. Lithium iodide salt (Aldrich, crystalline powder, 99.9% trace metals basis) as dopant was used and kept dry (in desiccator) before use.

### 2.2. Preparation of samples

**Table 1.** Designation of polymer electrolyte compositions.

Designation	RS:LiI (wt.%) Composition	Conductivity, $\sigma$ ( $\text{S cm}^{-1}$ )
RS-0	100:0	$6.87 \times 10^{-10}$
RS-1	95:5	$1.87 \times 10^{-8}$
RS-2	90:10	$3.33 \times 10^{-8}$
RS-3	85:15	$1.66 \times 10^{-8}$
RS-4	80:20	$1.59 \times 10^{-7}$
RS-5	75:25	$2.47 \times 10^{-6}$
RS-6	70:30	$3.83 \times 10^{-6}$
RS-7	65:35	$4.68 \times 10^{-5}$

Samples in form of film were prepared using conventional solution casting method. 1 g of rice starch was dissolved in 25 ml of DI-water as solvent for 15 min at 80 °C for gelatinization. After gelatinization the rice starch solution was allowed to cool down to room temperature, and LiI was added with different weight ratio according to Table 1. The mixtures were stirred to obtain fully dissolved and homogenous mixture. Consequently, samples were cast onto Teflon petri dishes and any residual solvent and water were evaporated in drying oven at 60 °C for 24 h. Dried solid films were cast and analysed directly at room temperature after drying procedure.

### 2.3. Characterization methods

#### 2.3.1 Impedance spectroscopy

Ionic conductivity and frequency dependency studies were carried out using electrochemical impedance spectroscopy (EIS) analyser, Hioki, 3532-50 LCR HiTESTER. The measurements were collected in frequency range of 50 Hz to 5 MHz. The samples were sandwiched between two stainless steel blocking electrodes with area of 2.98 cm<sup>2</sup>. Imaginary parts of impedance were automatically computed with LCR HiTESTER. Cole-Cole plots were used to determine bulk resistance ( $R_b$ ) to calculate ionic conductivity ( $\sigma$ ) using following equation:

$$\sigma = \frac{L}{R_b A} \quad (1)$$

where  $\sigma$  is in S cm<sup>-1</sup>,  $L$  and  $A$  are the thickness of sample and area of blocking electrodes, respectively. Thickness of samples was measured using Mitutoyo digital gauge.

#### 2.3.2 Fourier transform infrared (FTIR) spectroscopy

Structural properties were analysed using FTIR spectrometer (Thermo Scientific, Nicolet iS10). The wavenumbers region was between 4000 and 400 cm<sup>-1</sup> with 2 cm<sup>-1</sup> resolution. Nitrogen gas was used to blank FTIR in order to remove CO<sub>2</sub> and water from environment. Infrared spectra of samples were collected after background collection.

## 3. RESULTS

Fig. 1 illustrates the variation of ionic conductivity with different LiI content. Figure shows conductivity increases with addition of LiI salt. Conductivity after addition of more than 15 wt.% of LiI increases dramatically until 35 wt.% LiI. Above 35 wt.% LiI, casting films was not applicable and not easy to handle. Conductivities of samples are tabulated in Table 1. The highest ionic conductivity is  $4.68 \times 10^{-5}$  S cm<sup>-1</sup> for RS-7 film with 75:35 wt.% of RS:LiI polymer electrolyte at room temperature.

To analyse mechanism of ionic conduction and related model the temperature-dependent ionic conductivity measurement was carried out. Fig. 2 demonstrates the log  $\sigma$  versus 1000/T for various

samples of RS-0, RS-5, RS-6 and RS-7 in temperature range from 303 K to 373 K. Results show that ionic conductivity increases with increase in temperature.

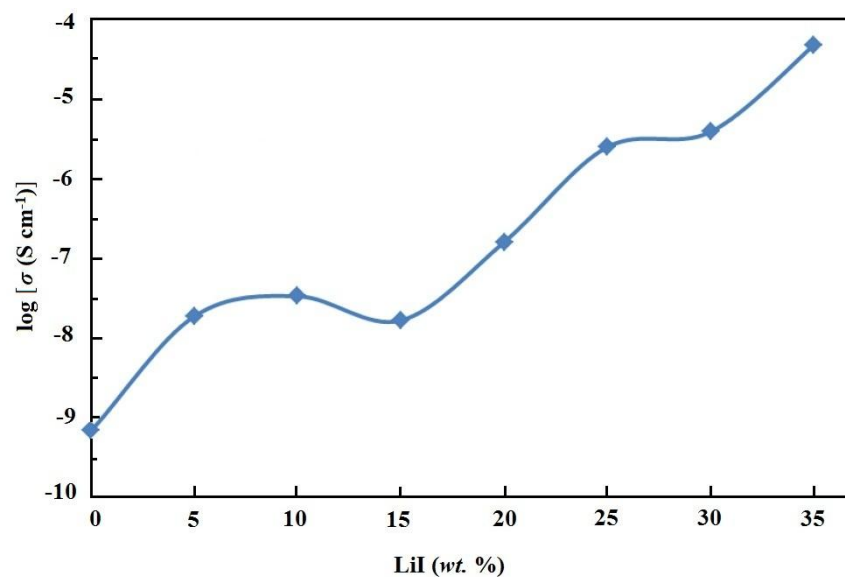


**Figure 1.** Conductivity of RS:LiI system in different LiI content at room temperature.

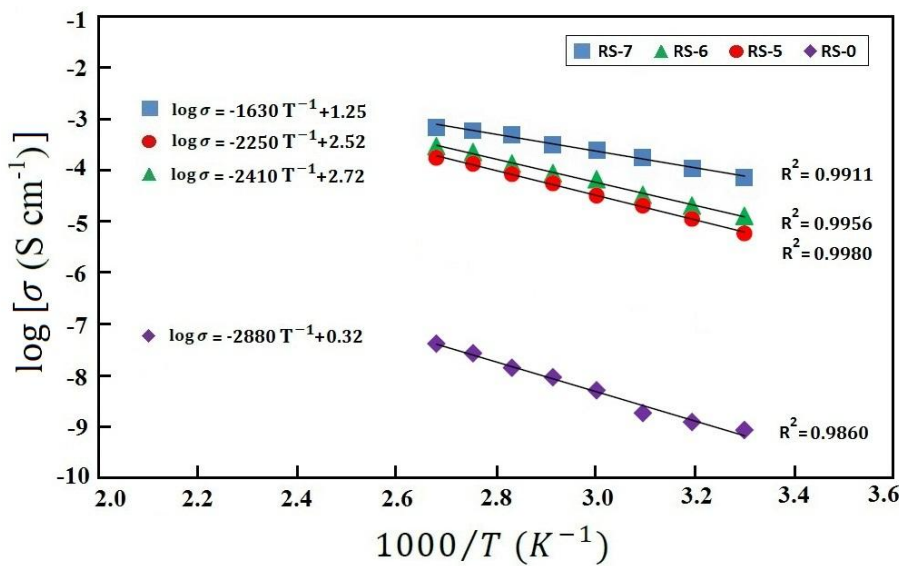


**Figure 2.** Temperature-dependence ionic conductivity of rice starch and lithium iodide system.

Fig. 3 shows variation of loss tangent with frequency for RS-7 (the highest conducting sample in the system) at different temperatures from 298 K to 373 K. Higher temperatures results in bigger peaks. The inset figure in Fig. 3 shows variation of relaxation time with LiI content for RS-0, RS-5, RS-6 and RS-7.

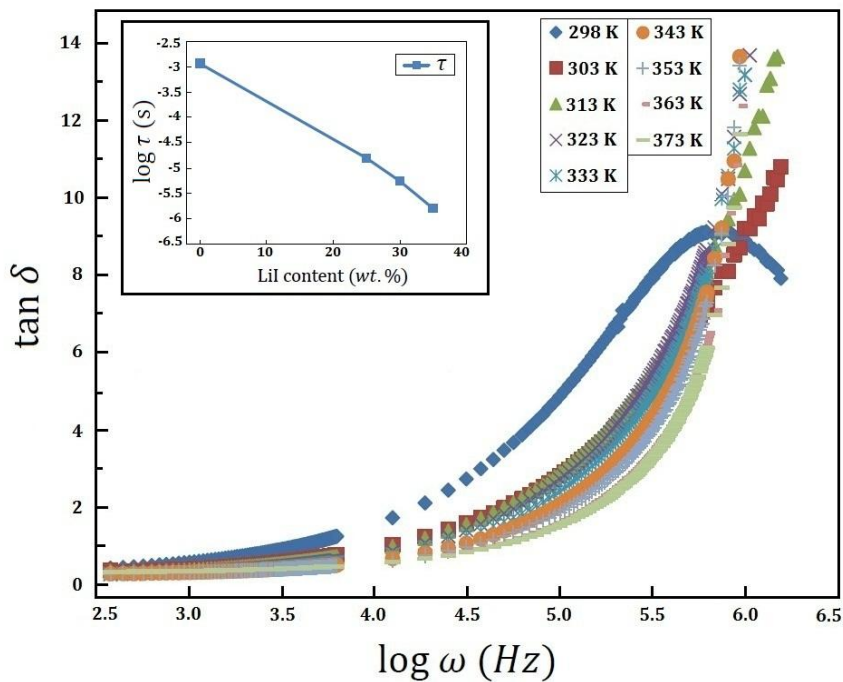


**Figure 3.** Variation of loss tangent with angular frequency for RS-7 at different temperatures from 298K to 373K. The inset figure exhibits variation of relaxation time for different LiI salt content.

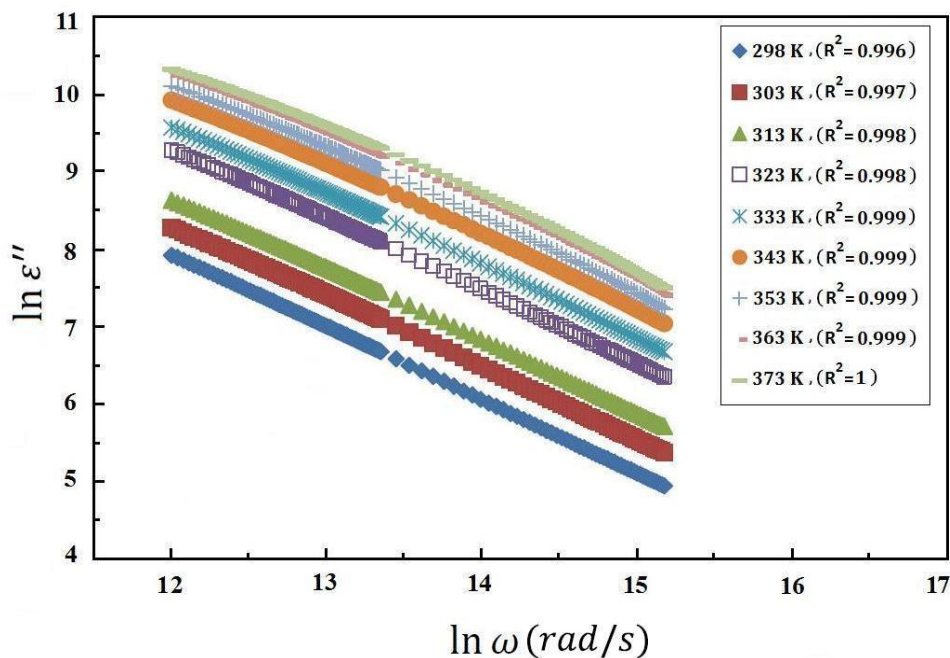


**Figure 4.**  $\ln \epsilon''$  versus  $\ln \omega$  at various temperatures for sample RS-7 as highest conductivity.

In ac-conductivity study, variation of  $\epsilon''$  with frequency was analysed in logarithmic scale. Fig. 4 shows  $\ln \epsilon''$  versus  $\ln \omega$  at different temperatures for RS-7. At Lower frequencies,  $\epsilon''$  is higher. The  $\epsilon''$  is decreased with increase in the frequency.

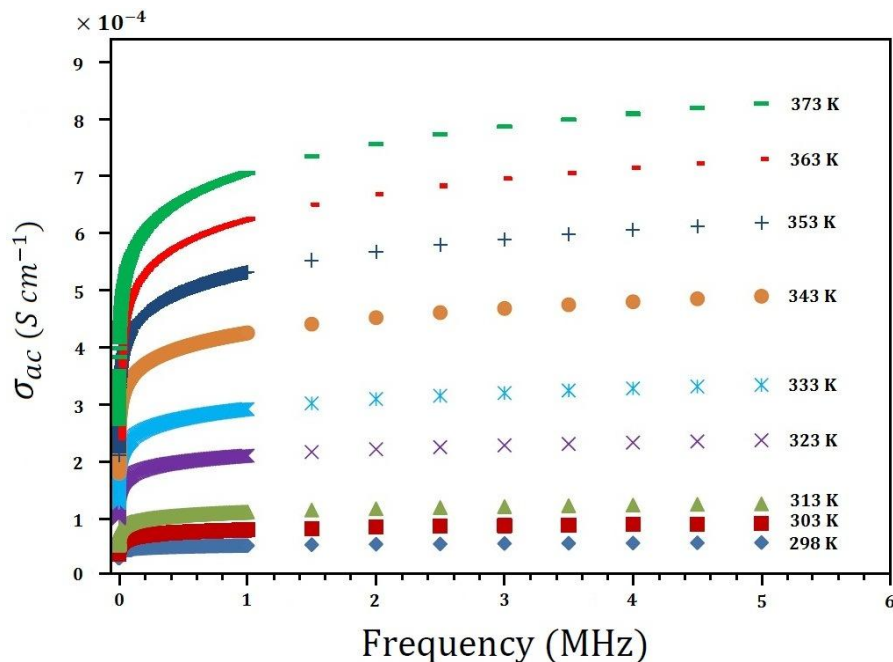


**Figure 5.** Variation of ac-conductivity with frequency range of 50 Hz to 5 MHz at different temperatures for RS-7.

Fig. 5 illustrates variation of ac-conductivity with frequency (5Hz to 5 MHz) at different temperatures for RS-7. Fig. 5 shows increase in ionic conductivity with increase in frequency and temperature.

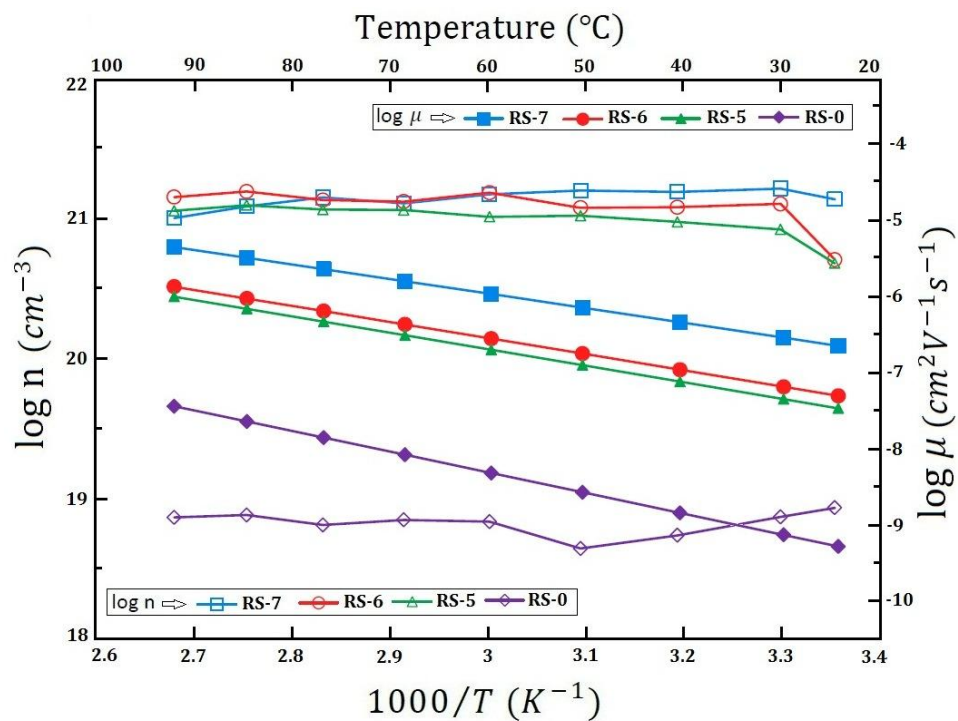
The logarithmic relaxation frequency ( $\log \omega_m$ ), activation energy ( $E_a$ ), free ion life-time ( $\tau_0$ ), mobility ( $\mu$ ), Diffusion coefficient ( $D$ ), the number density of mobile ions ( $n$ ) and the number of transitions per unit time ( $P(E)$ ) were calculated for RS-1, RS-2, RS-3, RS-4, RS-5, RS-6 and RS-7. These calculated transport parameters for RS-LiI system were illustrated in Table 2.

**Table 2.** Transport parameters for RS-LiI system.

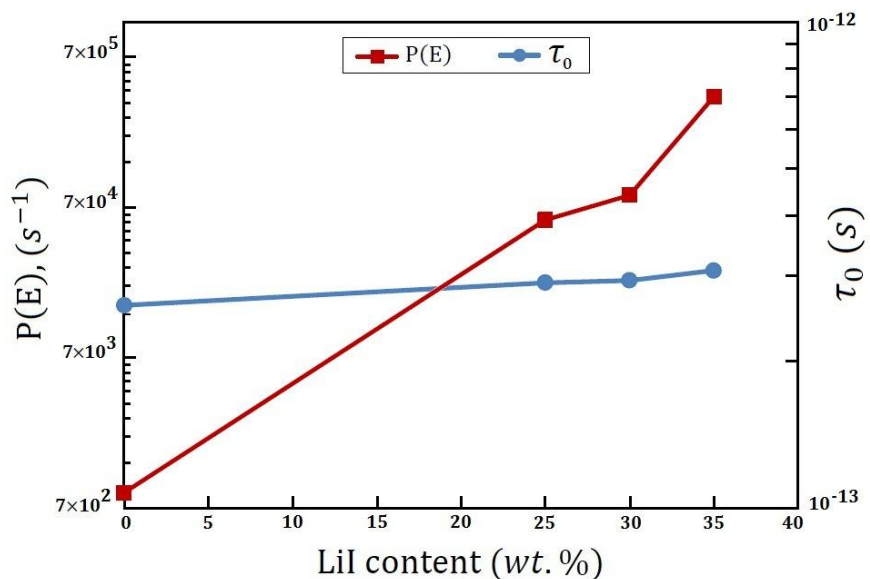
Samples	$\log \omega_m$ (Hz)	$E_a$ (eV)	$\tau_0 \times 10^{-13}$ (s)	$\mu$ (cm $^2$ V $^{-1}$ s)	$D$ (cm $^2$ s $^{-1}$ )	$n$ (cm $^{-3}$ )	$P(E)$ ,(s $^{-1}$ )
RS-1	2.88	0.54	2.68	$1.57 \times 10^{-9}$	$4.03 \times 10^{-11}$	$7.45 \times 10^{19}$	$2.80 \times 10^3$
RS-2	3.30	0.53(3)	2.70	$2.05 \times 10^{-9}$	$5.26 \times 10^{-11}$	$1.02 \times 10^{20}$	$3.65 \times 10^3$
RS-3	2.64	0.53(5)	2.69	$1.90 \times 10^{-9}$	$4.88 \times 10^{-11}$	$5.47 \times 10^{19}$	$3.38 \times 10^3$
RS-4	3.76	0.49	2.82	$1.05 \times 10^{-8}$	$2.69 \times 10^{-10}$	$9.50 \times 10^{19}$	$1.86 \times 10^4$
RS-5	4.80	0.46	2.91	$3.26 \times 10^{-8}$	$8.37 \times 10^{-10}$	$4.74 \times 10^{20}$	$5.80 \times 10^4$
RS-6	5.25	0.45	2.94	$4.75 \times 10^{-8}$	$1.22 \times 10^{-9}$	$5.04 \times 10^{20}$	$8.47 \times 10^4$
RS-7	5.79	0.41	3.08	$2.15 \times 10^{-7}$	$5.53 \times 10^{-9}$	$1.36 \times 10^{21}$	$3.83 \times 10^5$

Fig. 6 shows variation of the number density of mobile ions and mobility with temperature for samples RS-0, RS-5, RS-6 and RS-7. At room temperature the number density of mobile ions is

increasing with increase in salt content. Fig. 7 exhibits variation of the number of transitions and free ion life-time at different LiI content.



**Figure 6.** Variation of the number density of mobile ions and mobility with temperature for samples RS-0, RS-5, RS-6 and RS-7.



**Figure 7.** Variation of the number of transitions,  $P(E)$ , and the free ion life-time ( $\tau_0$ ) at different LiI content.

Fig. 8 shows FTIR spectra of RS-0, pure LiI, RS-5, RS-6 and RS-7. Shifts of Peaks at 1643, 1451 and 860 cm<sup>-1</sup> for pure rice starch (RS-0) confirms complexation between rice starch and LiI. Band assignments related to pure rice starch are tabulated in Table 3.

**Table 3.** Band assignments and infrared wavenumbers for pure rice starch.

Sample	Band assignment	Wavenumber (cm <sup>-1</sup> )
RS	O–H stretching (broad)	3310
	C–H <sub>2</sub> deformation (m) –(CH <sub>2</sub> )	2927
	H <sub>2</sub> O in amorphous regions of starch	1643
	C–H bending (v) - (CH <sub>2</sub> )	1451
	C–O–H bending , C–H twisting (CH <sub>2</sub> )	1337
	C–O stretching (s)	1150
	C–O–H bending (s)	1077
	C–H bending (v)	997
	Skeletal mode vibrations of α-1,4-glycosidic linkages, (C–O–C)	932
	C–H deformation	860
	C–C stretching (v)	760
note: RS= Rice Starch, (s)= strong, (m)= medium, (v)= variable		

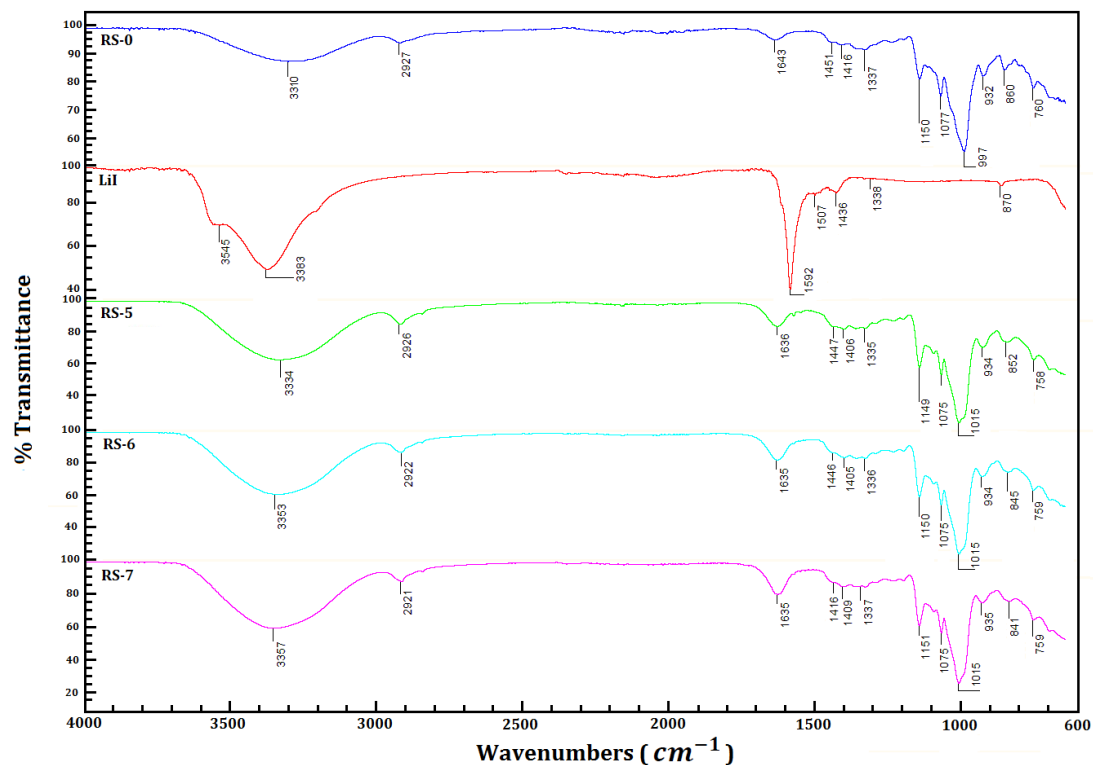


**Figure 8.** FTIR spectra of RS-0, pure LiI, RS-5, RS-6 and RS-7.

## 4. DISCUSSION

### 4.1. Ionic conductivity studies

#### 4.1.1. Effect of lithium iodide (LiI) content on conductivity

In this work, dependence of conductivity on lithium iodide concentration reveals effect of lithium iodide salt on conductivity after interaction with polymer. According to Fig. 1, it is confirmed that LiI content has direct effect on conductivity, which dramatically increase the conductivity in higher salt content. The reason is the number of  $\text{Li}^+$  mobile ions in lithium iodide salts as charge carriers. Increase in salt concentration cause increase in number of  $\text{Li}^+$  mobile ions.

#### 4.1.2. Temperature-dependent conductivity and loss tangent

The temperature-dependent conductivity study were investigated and demonstrated in Fig.2. Results confirm increase of ionic conductivity with increase in temperature. This is due to bond rotations which result in faster ion movements as temperature increases [56, 57]. Regressions ( $R^2 \sim 1$ ) show best confirmation of results lying on straight lines. According to Fig. 2 the temperature-dependence behaviour of RS:LiI system follows Arrhenius thermal activated model which expresses the relation between conductivity and temperature as

$$\sigma = \sigma_0 \exp\left[\frac{-E_a}{kT}\right] \quad (2)$$

Where  $\sigma_0$  is pre-exponential factor,  $E_a$  is activation energy and  $k$  is Boltzmann constant. Activation energies acquired from Eq. (1). Activation energy decreases with increase of conductivity which is related to increase of LiI content. Addition of salt produce more sites for ionic transport between conducting band and valence band which deduce to lower band gap as activation energy. This fact means ions in higher salt concentration (or higher conductivity) need less energy for transformation between transit sites. The mechanism is hopping  $\text{Li}^+$  ions on vacant places and increase in mobile ion numbers results in increase in conductivity [58].

Fig. 3 shows another temperature-dependent illustration related to loss tangent for highest conductivity film (RS-7). Loss tangent ( $\tan \delta$ ), were obtained following equation

$$\tan \delta = \frac{\varepsilon''}{\varepsilon'} \quad (3)$$

where  $\varepsilon'$  and  $\varepsilon''$  are the real and imaginary parts of complex permittivity ( $\varepsilon^* = \varepsilon' + i\varepsilon''$ ) known as dielectric constant and dielectric loss respectively. Using measured impedance values with EIS, real and imaginary parts of complex permittivity can be calculated from

$$\varepsilon' = \frac{Z''}{\omega C_0 (Z'^2 + Z''^2)} \quad (4)$$

$$\varepsilon'' = \frac{Z'}{\omega C_0 (Z'^2 + Z''^2)} \quad (5)$$

where  $Z'$  and  $Z''$  are real and imaginary parts of complex impedance. Here  $C_0 = \varepsilon_0 A/L$  represents vacuum capacitance related to electrodes and sample configuration,  $A$  is

surface area of blocking electrodes,  $L$  is thickness of sample, and  $\epsilon_0$  is the permittivity of the free space.

Fig. 3 demonstrates dependence of loss tangent on frequency in different temperatures. Loss tangent varies with any frequency change with peak caused by relaxation effect. At higher temperatures as conductivity increases, the peak in loss tangent shifts to higher magnitude with higher frequency. Moreover, bigger loss tangent (as a result of increase in conductivity and/or temperature) causes to shorten the relaxation time. This means ions transit faster between sites. Therefore, this displacement for loss tangent is due to fast ion movements in higher conductivity and temperature as a result of LiI addition, which is similar to temperature-dependence conductivity mechanism.

The inset in Fig. 3 exhibits variation of relaxation time ( $\tau$ ) with LiI content. The relaxation time decreases with increase in LiI content. This means increase in LiI content shorten the relaxation time which speeds up mobile ion transition and make higher conductivity.

#### 4.1.3. Frequency-dependent ac-conductivity

Ac-conductivity as part of total conductivity is important parameter which varies with frequency. Total conductivity is combination of dc and ac conductivities [59, 60]:

$$\sigma(\omega) = \sigma_{dc} + \sigma_{ac} = \sigma_{dc} + A\omega^s \quad (6)$$

and

$$\sigma_{ac} = A\omega^s \quad (7)$$

where  $A$  is a parameter dependent on temperature and  $s$  is the frequency exponent ( $<1$ ). To calculate ac-conductivity, parameter  $s$  should be calculated. On the other hand, for ac conductivity another equation is expressed as

$$\sigma_{ac} = \omega\epsilon_0\epsilon'\tan\delta \quad (8)$$

Substituting eq. (3) for  $\tan\delta$  in eq. (8) results in

$$\sigma_{ac} = \epsilon_0\epsilon''\omega \quad (9)$$

Finally, using eq. (7) and (9)

$$\epsilon_0\epsilon''\omega = A\omega^s \quad (10)$$

Hence

$$\epsilon'' = \frac{A}{\epsilon_0}\omega^{s-1} \quad (11)$$

This can be written as

$$\ln\epsilon'' = \ln\frac{A}{\epsilon_0} + (s-1)\ln\omega \quad (12)$$

Fig. 4 exhibits  $\ln\epsilon''$  versus  $\ln\omega$  at various temperatures for sample RS-7. This graph shows most straight lines according to regressions ( $R^2 \sim 1$ ) which can satisfy Eq. (12) to obtain parameter  $s$  from the slope of  $\ln\epsilon''$  versus  $\ln\omega$ . At room temperature ac-conductivity for RS-7 found to be

$$\sigma_{ac} = 1.92 \times 10^{-5} \omega^{0.061} \quad (13)$$

where  $s$  and  $A$  are calculated from eq. (12) using information from Fig. 4. Fig. 5 demonstrates variation of ac-conductivity with frequency at different temperatures for RS-7. The figure shows

sudden increase of ac-conductivity at low frequencies. At higher frequencies  $\sigma_{ac}$  reaches to a saturation value. In all frequency ranges,  $\sigma_{ac}$  increases with increase in temperature. This figure reveals that  $\sigma_{ac}$  is frequency and temperature dependent similar to dc conductivity. Higher ionic conductivities obtained at higher frequencies. Moreover, dependence of ac-conductivity on frequency is expressed in relation between  $\sigma_{ac}$  and frequency in Eqs. (7) and (9) which confirms experimental results in Fig. 5.

#### 4.1.4. Ionic transport parameters

Ionic transport mechanism in solid polymer electrolytes, can be expressed by the Rice and Roth [61] model. This model shows the ionic conductivity of mobile ions has relation with some other transport parameters as

$$\sigma = \frac{2}{3} \left[ \frac{(Ze)^2}{kTm} \right] n E_a \tau_0 \exp\left(-\frac{E_a}{kT}\right) \quad (14)$$

where  $Ze$  denotes the charge carried by an ion belonging to the conducting species which  $Z$  is valency of ion,  $k$  is Boltzmann constant,  $m$  is mass of ionic carrier,  $n$  is the number density of mobile ions,  $\tau_0$  is the free ion life-time.  $\tau_0$  was obtained from the mean free pass relation expressed by ( $\ell = v\tau_0$ ),  $v$  is velocity of the free ions ( $= \sqrt{2E/m}$ ). Here, mean free path ( $\ell$ ) for rice starch is distance between two repeating unit of amylose which found 10.4 Å [62]. The starch is composed of amylose and amylopectin, but we chose amylose for mean free path calculation rather than amylopectin. The reason can be expressed as amylose has  $\alpha$ -1,4-glucosidic linkages and amylopectin has  $\alpha$ -1,6-glucosidic linkages. Thus, the attachment of mobile ions to the amylose compound is easier than the amylopectin. Because  $\alpha$ -1,4-glucosidic linkages in amylose is more stable and less steric than the  $\alpha$ -1,6-glucosidic linkages in amylopectin. This reason is the branching structure in amylopectin has greater steric hindrance and thus prevents chemical reactions rather than the linear structure of the amylose [63].

Moreover, using Eq. (14) the number density of mobile ions can be calculated. Other transport parameters such as mobility ( $\mu$ ) and diffusion coefficient ( $D$ ) can be obtained from relationship between mobility and conductivity, and from Einstein relation with determinate value of  $n$  and  $\sigma$  as expressed below:

$$\mu = \frac{\sigma}{ne} \quad (15)$$

and

$$D = \frac{kT\sigma}{ne^2} \quad (16)$$

where  $D$  is diffusion coefficient and  $e$  is electronic charge. Calculated transport parameters are depicted in Table 2. Results from Table 2 show that the ionic conductivity increases with increase in the number density of mobile ions. This is due to effect of LiI salt addition. Also increase in the number density of mobile ions results in increase of the relaxation frequency, mobility and diffusion coefficient.

Fig. 6 exhibits the variation of number density of mobile ions and mobility with temperature for samples RS-0, RS-5, RS-6 and RS-7. The number density of mobile ions increases at lower temperature. At higher temperatures there are fluctuations but there is no dramatic change. The mobility is increasing in all temperatures from 298 to 373 K.

Another transport parameter investigated in this work is the number of transitions per unit time,  $P(E)$ , which denoted by equation below [61]

$$P(E) = \frac{1}{\tau_0} \exp\left(\frac{-E_a}{kT}\right) \quad (17)$$

where  $\tau_0$  is free ion life-time and  $E_a$  is activation energy. Fig. 7 shows variation of the number of transitions and free ion life-time ( $\tau_0$ ) with LiI salt content. The number of transitions increases dramatically with increase in LiI salt content. This further confirms the effect of  $\text{Li}^+$  mobile ions resulting from LiI salt content on conductivity and transport parameters including the number of transitions.

#### 4.2. FTIR analysis

The FTIR analysis of polymer electrolytes is important factor to monitor polymer and salt complexation, ion-ion and ion-polymer interactions as a function of salt concentration [64]. In this work the complexation between RS and LiI salt was investigated using FTIR spectroscopy.

Fig. 8 represents FTIR spectra of RS-0, RS-5, RS-6, RS-7 and pure LiI salt at different wavenumbers between 4000 and 400  $\text{cm}^{-1}$ . The important band assignments for pure rice starch (RS-0) are represented in Table 3 [65, 66].

In Fig. 8, the peak of 1643  $\text{cm}^{-1}$  for pure RS (RS-0) is shifted to lower frequencies of 1636 and 1635  $\text{cm}^{-1}$  for RS-5 and RS-7 respectively due to influence of the peak in LiI salt, which is evidence of complexation between rice starch polymer and LiI salt. Moreover, the peak at 1451  $\text{cm}^{-1}$  in pure RS characteristic of C-H bending ( $\text{CH}_2$ ), is shifted to lower frequencies at 1447, 1446 and 1416  $\text{cm}^{-1}$  in RS-5, RS-6 and RS-7 respectively expressing complexation with LiI salt. In lower frequency range there is also evidence of complexation at peak of C-H bond at 860  $\text{cm}^{-1}$  which is shifted to lower frequencies of 852, 845 and 841  $\text{cm}^{-1}$  in RS-5, RS-6 and RS-7 respectively.

## 5. CONCLUSION

Polymer electrolytes based on biodegradable rice starch and lithium iodide were prepared and complexation between rice starch and lithium iodide occurred. The temperature-dependence study of the ionic conductivity obeys Arrhenius model. Transport parameters were studied with Rice and Roth model. Lithium iodide contents with  $\text{Li}^+$  mobile ions effect directly on transport parameters and ionic conductivity. Addition of LiI results in increase of the number density of mobile ions which is main reason to increase and enhancement of ionic conductivity. Highest conductivity was achieved at  $4.68 \times 10^{-5} \text{ S cm}^{-1}$ . The ac-conductivity increased at higher frequency and temperatures. The shift in

loss tangent to higher frequency causes to decrease and shorten the relaxation time to fasten transitions which is increase the number of transitions and subsequently increasing the ionic conductivity.

## ACKNOWLEDGEMENTS

M. H. Khanmirzaei acknowledges the Universiti Malaya Bright Sparks Scheme (SBSUM) for the financial support (BSP 221(3)-12). This work was supported by the University of Malaya Research Grant (UMRG Program: RP001-2013A) and PPP Grant (PG105-2012B).

## References

1. S. Aoyagi, H. Izumi, S. Nakahara, M. Ochi and H. Ogawa, *Sens. Actuator A-Phys.*, 145–146 (2008) 464.
2. H. Tian, Z. Tang, X. Zhuang, X. Chen and X. Jing, *Prog. Polym. Sci.*, 37 (2012) 237.
3. L.S. Nair and C.T. Laurencin, *Prog. Polym. Sci.*, 32 (2007) 762.
4. S. Sinha Ray and M. Bousmina, *Prog. Mater. Sci.*, 50 (2005) 962.
5. I. Armentano, M. Dottori, E. Fortunati, S. Mattioli and J.M. Kenny, *Polym. Degrad. Stabil.*, 95 (2010) 2126.
6. E. Leclerc, F. Miyata, K.S. Furukawa, T. Ushida, Y. Sakai and T. Fujii, *Mater. Sci. Eng. C-Mater. Biol. Appl.*, 24 (2004) 349.
7. K. Imasaka, M. Yoshida, H. Fukuzaki, M. Asano, M. Kumakura, T. Mashimo, H. Yamanaka and T. Nagai, *Int. J. Pharmaceut.*, 81 (1992) 31.
8. L. Xu and A. Yamamoto, *Colloid surf. B-Biointerfaces*, 93 (2012) 67.
9. P. Gunatillake, R. Mayadunne, R. Adhikari, Recent developments in biodegradable synthetic polymers, in: M.R. El-Gewely (Ed.) *Biotechnology Annual Review*, Elsevier, (2006), pp. 301.
10. M. Schnabelrauch, S. Vogt, Y. Larcher and I. Wilke, *Biomolecular Engineering*, 19 (2002) 295.
11. J.C. Middleton and A.J. Tipton, *Biomaterials*, 21 (2000) 2335.
12. E. Leclerc, K.S. Furukawa, F. Miyata, Y. Sakai, T. Ushida and T. Fujii, *Biomaterials*, 25 (2004) 4683.
13. M. Kim, B. Jung and J.-H. Park, *Biomaterials*, 33 (2012) 668.
14. N. Nishat and A. Malik, Biodegradable coordination polymer: Polycondensation of glutaraldehyde and starch in complex formation with transition metals Mn(II), Co(II), Ni(II), Cu(II) and Zn(II), *Arabian Journal of Chemistry*.
15. A. Boley, W.R. Müller and G. Haider, *Aquac. Eng.*, 22 (2000) 75.
16. G. Winzenburg, C. Schmidt, S. Fuchs and T. Kissel, *Adv. Drug Deliv. Rev.*, 56 (2004) 1453.
17. Y. Lu and S.C. Chen, *Adv. Drug Deliv. Rev.*, 56 (2004) 1621.
18. S. Lakshmi, D.S. Katti and C.T. Laurencin, *Adv. Drug Deliv. Rev.*, 55 (2003) 467.
19. C.P. Fonseca and S. Neves, *J. Power Sources*, 159 (2006) 712.
20. C.P. Fonseca, D.S. Rosa, F. Gaboardi and S. Neves, *J. Power Sources*, 155 (2006) 381.
21. Y.S. Zhu, X.J. Wang, Y.Y. Hou, X.W. Gao, L.L. Liu, Y.P. Wu and M. Shimizu, *Electrochim. Acta*, 87 (2013) 113.
22. M. Strange, D. Plackett, M. Kaasgaard and F.C. Krebs, *Sol. Energ. Mat. Sol. C.*, 92 (2008) 805.
23. R. Singh, N.A. Jadhav, S. Majumder, B. Bhattacharya and P.K. Singh, *Carbohyd. Polym.*, 91 (2013) 682.
24. Y.N. Sudhakar and M. Selvakumar, *Electrochim. Acta*, 78 (2012) 398.
25. B.P. Tripathi and V.K. Shahi, *Prog. Polym. Sci.*, 36 (2011) 945.
26. X.Y. Wang, X.X. Li, L. Chen, F.W. Xie, L. Yu and B. Li, *Food Chem.*, 126 (2011) 1218.
27. H.C. Pu, Ling Li, Xiaoxi Xie, Fengwei Yu, Long Li and Lin, *J. Agric. Food Chem.*, 59 (2011) 5738.

28. M.R. Saboktakin, Tabatabaie, R.M., Maharramov, A. and Ramazanov, M.A., *Int. J. Biol. Macromol.*, 48 (2010) 381.
29. P. De Koninck, D. Archambault, F. Hamel, F. Sarhan and M.A. Mateescu, *J. Pharm. Pharm. Sci.*, 13 (2010) 78.
30. M. Lemieux, P. Gosselin and M.A. Mateescu, *Int. J. Pharmaceut.*, 382 (2009) 172.
31. G. Sen and S. Pal, *J. Appl. Polym. Sci.*, 114 (2009) 2798.
32. F. Brouillet, B. Bataille and L. Cartilier, *Int. J. Pharmaceut.*, 356 (2008) 52.
33. I. Arvanitoyannis, C.G. Biliaderis, H. Ogawa and N. Kawasaki, *Carbohydr. Polym.*, 36 (1998) 89.
34. D.B.V.E. Emeje Martins Ochubiojo and Asha Rodrigues, Starch: From food to Medicine, (Ed.) *Scientific, Health and Social Aspects of the Food Industry*, InTech, (2012).
35. R.F.M.S. Marcondes, P.S. D'Agostini, J. Ferreira, E.M. Girotto, A. Pawlicka and D.C. Dragunski, *Solid State Ion.*, 181 (2010) 586.
36. S. Ramesh, R. Shanti and E. Morris, *J. Mol. Liq.*, 166 (2012) 40.
37. R.I. Mattos, C.E. Tambelli, J.P. Donoso and A. Pawlicka, *Electrochim. Acta*, 53 (2007) 1461.
38. L.V.S. Lopes, D.C. Dragunski, A. Pawlicka and J.P. Donoso, *Electrochim. Acta*, 48 (2003) 2021.
39. S. Ramesh, R. Shanti and E. Morris, *Carbohydr. Polym.*, 87 (2012) 701.
40. W. Ning, Z. Xingxiang, L. Haihui and W. Jianping, *Carbohydr. Polym.*, 77 (2009) 607.
41. W. Ning, Z. Xingxiang, L. Haihui and H. Benqiao, *Carbohydr. Polym.*, 76 (2009) 482.
42. M. Kumar, T. Tiwari and N. Srivastava, *Carbohydr. Polym.*, 88 (2012) 54.
43. Y. Viturawong, P. Achayuthakan and M. Suphantharika, *Food Chem.*, 111 (2008) 106.
44. H. Yamamoto, N. Isozumi and T. Sugitani, *Carbohydr. Polym.*, 62 (2005) 379.
45. H.H. Shaarawy, S.M. El-Rafie, A.M. Abd El-Ghaffar and M.H. El-Rafie, *Carbohydr. Polym.*, 75 (2009) 208.
46. W. Samutsri and M. Suphantharika, *Carbohydr. Polym.*, 87 (2012) 1559.
47. B. Heyman, D. De Hertogh, P. Van der Meer, F. Depypere and K. Dewettinck, *Carbohydr. Polym.*
48. M.L. Kaplan, E.A. Reitman and R.J. Cava, *Polymer*, 30 (1989) 504.
49. M.S. Su'ait, A. Ahmad, H. Hamzah and M.Y.A. Rahman, *Electrochim. Acta*, 57 (2011) 123.
50. K. Kiran Kumar, M. Ravi, Y. Pavani, S. Bhavani, A.K. Sharma and V.V.R. Narasimha Rao, *Physica B*, 406 (2011) 1706.
51. N. Kobayashi, S. Sunaga and R. Hirohashi, *Polymer*, 33 (1992) 3044.
52. J. Nei de Freitas, C. Longo, A.F. Nogueira and M.-A. De Paoli, *Sol. Energ. Mat. Sol. C.*, 92 (2008) 1110.
53. M. Cho, H. Seo, J. Nam, H. Choi, J. Koo and Y. Lee, *Sens. Actuators B-Chem.*, 128 (2007) 70.
54. N.-S. Choi, B. Koo, J.-T. Yeon, K.T. Lee and D.-W. Kim, *Electrochim. Acta*, 56 (2011) 7249.
55. D. Wei, *Int. J. Mol. Sci.*, 11 (2010) 1103.
56. C.V. Subba Reddy, A.K. Sharma and V.V.R. Narasimha Rao, *J. Power Sources*, 114 (2003) 338.
57. R. Baskaran, S. Selvasekarapandian, G. Hirankumar and M.S. Bhuvaneswari, *Ionics*, 10 (2004) 129.
58. T. Uma, T. Mahalingam and U. Stimming, *Mater. Chem. Phys.*, 82 (2003) 478.
59. N.F. Mott and E.A. Davis, *Electronic processes in non-crystalline materials*, 2d ed., Clarendon Press; Oxford (1979).
60. S.R. Elliott, *Adv. Phys.*, 36 (1987) 135.
61. M.J. Rice and W.L. Roth, *J. Solid State Chem.*, 4 (1972) 294.
62. H.W. Hsein-Chih and A. Sarko, *Carbohydr. Res.*, 61 (1978) 7.
63. A.S.A. Khiar and A.K. Arof, *Ionics*, 16 (2010) 123.
64. S. Selvasekarapandian, R. Baskaran, O. Kamishima, J. Kawamura and T. Hattori, *Spectroc. Acta Pt. A-Molec. Biomolec. Spectr.*, 65 (2006) 1234.
65. R. Kizil, J. Irudayaraj and K. Seetharaman, *J. Agric. Food Chem.*, 50 (2002) 3912.

66. E. Pretsch, P. Buhlmann and M. Badertscher, *Structure determination of organic compounds : tables of spectral data*, 4th, rev. and enl. ed., Springer, Berlin, (2009).